

PAPER • OPEN ACCESS

## Electronic transport in high magnetic fields of thin film MnSi

To cite this article: N Steinki *et al* 2020 *J. Phys. Commun.* **4** 035008

View the [article online](#) for updates and enhancements.



## PAPER

## Electronic transport in high magnetic fields of thin film MnSi

N Steinki<sup>1</sup>, D Schroeter<sup>1</sup>, N Wächter<sup>1</sup>, D Menzel<sup>1</sup>, H W Schumacher<sup>2</sup>, I Sheikin<sup>3</sup> and S Süllo<sup>1</sup> <sup>1</sup> Institut für Physik der Kondensierten Materie, Technische Universität Braunschweig, Mendelssohnstr. 3, 38106 Braunschweig, Germany<sup>2</sup> Physikalisch-Technische Bundesanstalt, 38116 Braunschweig, Germany<sup>3</sup> Laboratoire National des Champs Magnétiques Intenses (LNCMI-EMFL), CNRS, UGA, 38042 Grenoble, FranceE-mail: [s.suellow@tu-bs.de](mailto:s.suellow@tu-bs.de)**Keywords:** magnetic order, magnetotransport, spin dynamics

## OPEN ACCESS

## RECEIVED

28 November 2019

## REVISED

25 February 2020

## ACCEPTED FOR PUBLICATION

2 March 2020

## PUBLISHED

9 March 2020

Original content from this work may be used under the terms of the [Creative Commons Attribution 4.0 licence](#).

Any further distribution of this work must maintain attribution to the author(s) and the title of the work, journal citation and DOI.



## Abstract

We present a study of the magnetoresistivity of thin film MnSi in high magnetic fields. We establish that the magnetoresistivity can be understood in terms of spin fluctuation theory, allowing us to compare our data to studies of bulk material. Despite of a close qualitative resemblance of bulk and thin film data, there are clear quantitative differences. We propose that these reflect a difference of the spin fluctuation spectra in thin film and bulk material MnSi, and discuss possible causes.

## 1. Introduction

The cubic helimagnet MnSi has intrigued researchers in the field of solid state magnetism for over half a century [1–3]. The material, belonging to the class of *B20* compounds, was originally studied in the context of spin fluctuation theory [4, 5]. Later, the pressure induced suppression of helical magnetic order ( $T_N = 29$  K at ambient pressure) became the focus of studies in the context of quantum criticality in itinerant *d*-metals [3, 6]. Finally, it was noted that the early-reported field-induced A-phase in MnSi [4] does represent a skyrmion lattice phase [7], this way establishing the material as a model compound for studies of skyrmion physics.

Especially in the latter context of skyrmionics, in recent years various efforts have been undertaken to grow MnSi thin films. Conceptually, the idea is based on the notion that skyrmionic phases should be energetically favored in two-dimensional structures. Hence, in order to study skyrmionic properties in solid state materials, thin film MnSi has been a prominent candidate to perform corresponding studies [8–29]. Surprisingly, while these studies brought various insights into the relationship of the properties of thin film MnSi and the corresponding bulk behavior, there are also a few quite striking differences.

First of all, in comparison to bulk material, thin film MnSi undergoes a transition into a helical magnetic phase below  $T_N \sim 45$  K [8–29]. This enhanced  $T_N$  is attributed to the tensile strain in the MnSi film, exerted by the mismatch of the lattice parameters of MnSi and the underlying Si substrate. Effectively, it leads to a state of negative pressure in thin film material, with the bulk  $T_N$  recovered if the films are pressurized [20].

Moreover, the structural anisotropy induced by the tensile strain affects the in-field properties, leading for instance to an increased critical field  $B_C$  into the magnetically polarized state [16]. Most strikingly, as yet there is no direct experimental evidence for a skyrmion lattice phase for the so-called out-of-plane geometry in thin film MnSi. As well, there is no final consensus if this ‘non-observation’ of a skyrmion lattice is an intrinsic or extrinsic property. On the one hand, it was argued that the effective negative pressure and pressure induced anisotropy drives thin film MnSi into a parameter range where a skyrmion lattice would not be stable anymore [10]. On the other hand, the thin films—even if grown epitaxially—arise from island growth on the Si substrate. This results in merohedrally twinned thin films, i.e., the films contain left- and right-handed crystallites. In this situation, the corresponding skyrmions would have opposite sense of rotation, and would annihilate upon meeting. Here, the lack of observation of a skyrmion lattice would be extrinsic, as it results from the non-mono-chiral character of the films.

The difference in behavior of thin film and bulk MnSi begs the question if they can be related to fundamental material properties. Bulk MnSi is a prime example of a system, where spin fluctuation theory has been invoked to quantitatively describe the material properties. An analogous study of thin film MnSi seems worthwhile, with

issues such as the influence of residual disorder in the films, structural low- (two)-dimensionality or the effectively negative pressure possibly becoming relevant. Therefore, we have set out to perform a high field magnetoresistivity study of thin film MnSi. In our approach, we closely follow in procedure and compare our data to a seminal study of the magnetoresistive properties of bulk single crystalline MnSi [4]. Based on the comparison, we discuss the electronic properties of thin film MnSi in terms of spin fluctuation theory.

## 2. Experimental

For the high magnetic field studies, two epitaxial grown MnSi thin films (thickness sample #1: 10 nm; sample #2: 30 nm) were synthesized by molecular beam epitaxy on [111] Si-substrate as described previously [29]. Previously, we have extensively characterized thin films MnSi produced in this manner both structurally and magnetically by various experimental techniques such as RHEED, TEM, AFM, magnetization/susceptibility and resistivity [13, 16, 20, 29]. Regarding their structural properties, the thin films form as layers of preferentially oriented MnSi domains, reflecting an island like growth process of the films. The lateral domain size is determined to the order of up to 100 nm, while the films are flat with a roughness  $\sim 1$  nm. The magnetic properties of the films have been established to fully correspond to those reported for instance in the [8, 12, 20], where evidence has been presented that tensile strain substantially affects the properties of thin film MnSi. To enable a direct comparison between MnSi thin films and MnSi bulk material regarding the magnetotransport properties the MnSi thin film samples were micro-structured by electron beam lithography (see [29]). This allows resistance measurements with a conventional four point AC-method in the same geometry as for bulk material. The structures are  $50\ \mu\text{m}$  wide and the voltage leads have a distance of  $70\ \mu\text{m}$ .

The high magnetic field measurements were performed on the thin film samples at the Laboratoire National des Champs Magnétiques Intenses in Grenoble, France. The magnetoresistivity was measured at various temperatures in a range between 3 and 100 K in an external magnetic field  $B$  up to 24 T. For both samples the external magnetic field was applied perpendicular and parallel to the sample current ( $B \perp I$  and  $B \parallel I$ ). In the former configuration, the field was applied out-of-plane, in the latter in-plane.

For direct comparison to the results from [4], we also studied MnSi bulk crystals synthesized by the Czochralski tri-arc method. The single crystals have been characterized with respect to their essential physical properties as described below. The transverse magnetoresistivity ( $B \perp I$ ) of the bulk samples was determined in a temperature range between 2 and 100 K in an external magnetic field up to 8 T. In addition the zero field resistivity of all samples was measured in a temperature range between 2 and 300 K.

## 3. Results

In figure 1 we plot the zero field resistivities of our bulk and thin film samples. Qualitatively, the overall behavior is similar to that reported previously for single-crystalline and thin film material. For both types of systems, overall there is a metallic temperature dependence, with an anomaly at the transition at  $T_N$  into the helical state, a  $T^2$ -like behavior below  $T_N$  and some rounding of the resistivity above  $T_N$  attributed to spin fluctuations on top of the phononic resistivity. In detail, however, there are a few issues to be noted.

First, while all single crystals MnSi have the same transition temperature  $T_N = 29$  K into the helimagnetic state (also verified by susceptibility measurements, not shown) and exhibit a similar temperature dependence of the resistivity  $\rho$ , absolute values of  $\rho$  vary by more than an order of magnitude. It suggests that the determination of the absolute value of  $\rho$  is affected by cracks in the single crystalline samples. Then, in terms of characterizing the crystalline quality of our bulk samples, instead of the residual resistivity  $\rho_0$  the best measure is the residual resistivity ratio (RRR) here defined as  $\rho_{300\text{K}}/\rho_{2\text{K}}$ . We find values RRR for sample #3: RRR=15, #4: RRR = 42 and #5: RRR = 104. We thus conclude that sample #5 has the highest crystalline quality, even though the room temperature resistivity is nonphysically high with  $1700\ \mu\Omega\text{cm}$ . For comparison, from the experimental data published in [4] we estimate a value RRR for the crystal studied in that work of the order of 60. Nowadays, for MnSi, in general a RRR of the order of 100 is taken to signal a ‘good sample quality’ [30].

Second, for the thin film samples we find transition temperatures  $T_N = 45$  K into the helimagnetic state, consistent with previous reports [8–29]. Only, at high temperatures both film samples exhibit a downturn of  $\rho$ , different from the single crystal behavior. As we have demonstrated in [29], the downturn arises from a breakdown of a Schottky barrier between thin film MnSi and the Si substrate. In result, at high temperatures the MnSi film is shortcut by the substrate, leading to the downturn in  $\rho$ . We note that—while we need to keep aware of these experimental artifacts—they will not affect the magnetoresistive behavior reported below, as we can use normalized representations of the magnetoresistive behavior and we discuss only low-temperature data not affected by the shortcut.

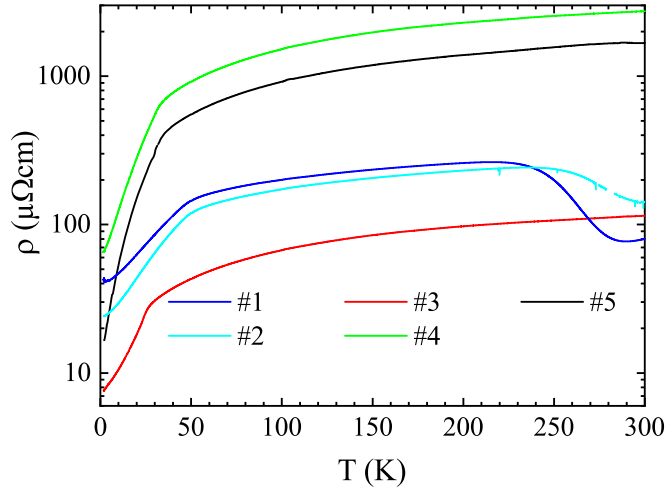


**Figure 1.** Zero field resistivity of different samples MnSi (#1: thin film 10 nm thickness, #2: thin film 30 nm thickness, #3: bulk with RRR of 15, #4: bulk with RRR of 42, #5: bulk with RRR of 104); for details see text.

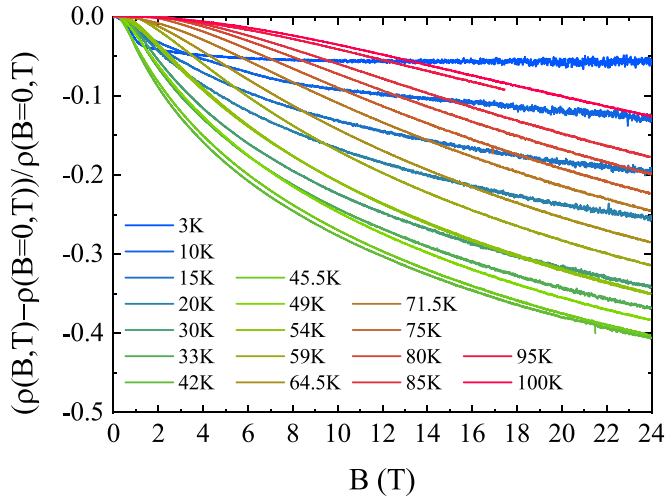


**Figure 2.** Magnetoresistivity in transverse magnetic fields up to 24 T for a 30 nm thin film MnSi; for details see text.

Subsequently, we have carried out an extensive run of magnetoresistivity measurements. As an example, in figure 2 we plot the magnetoresistivity  $MR$  defined as  $MR = (\rho(B, T) - \rho(B = 0, T)) / \rho(B = 0, T)$  in transverse magnetic fields  $B$  up to 24 T at temperatures between 3 and 100 K for the 30 nm thick sample MnSi. Qualitatively and semiquantitatively, as will be documented below, the general behavior reported here for the 30 nm sample in transverse geometry is similarly seen for the 10 nm sample and the second field alignment.

For low temperatures, the magnetoresistivity exhibits an inverted S-shaped behavior which is easily saturated in a few T. As temperature is increased up to  $T_N$ , the  $MR$  increases as well and the inverted S-shaped behavior broadens without reaching saturation. Finally, above  $T_N$  only the downward curvature of the  $MR \propto B^2$  remains from the inverted S-shaped character, with the overall size of the  $MR$  being reduced again relative to the signal close to  $T_N$  in the field range covered.

From the data presented in figure 2, to directly compare to [4] we construct the temperature dependence of  $\rho$  in transverse magnetic fields up to 24 T for the 30 nm thick sample MnSi (plotted in figure 3). Qualitatively, the behavior is similar to that reported in [4] (see figure 6 therein), with a suppression of the resistivity in magnetic fields over a wide temperature range and the largest effect close to  $T_N$ . We note that the critical field of the helical phase of MnSi is about 1 T, accounting for the observed disappearance of the kink in the resistivity in the magnetic fields plotted here. Of course, the qualitative similarity in behavior of single crystal and thin film material holds as well for the measurements of the 10 nm sample and the second field alignment (not shown).

The interpretation of the magnetoresistivity of MnSi has invoked the suppression of spin fluctuations in magnetic fields. These spin fluctuations are present over a very wide temperature range. A different approach to

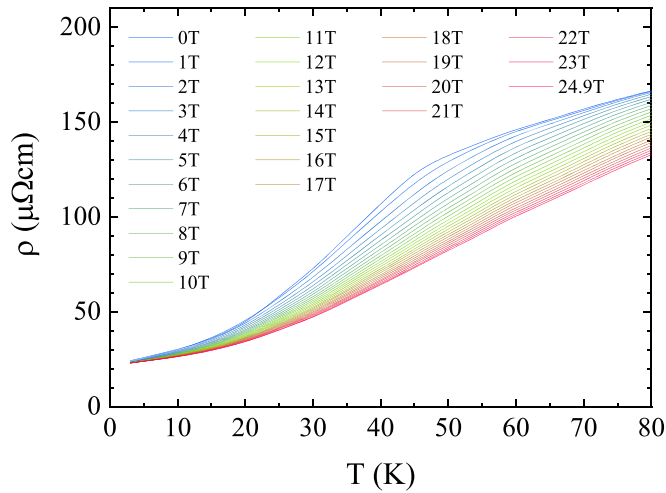


**Figure 3.** Resistivity in transverse magnetic fields up to 24 T for a 30 nm thin film MnSi; for details see text.

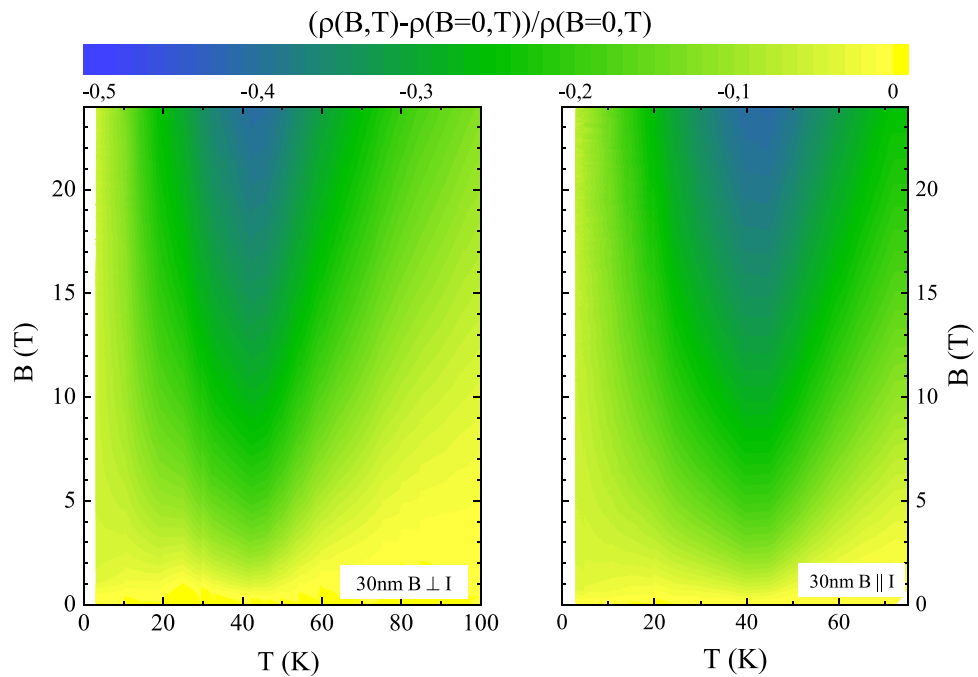
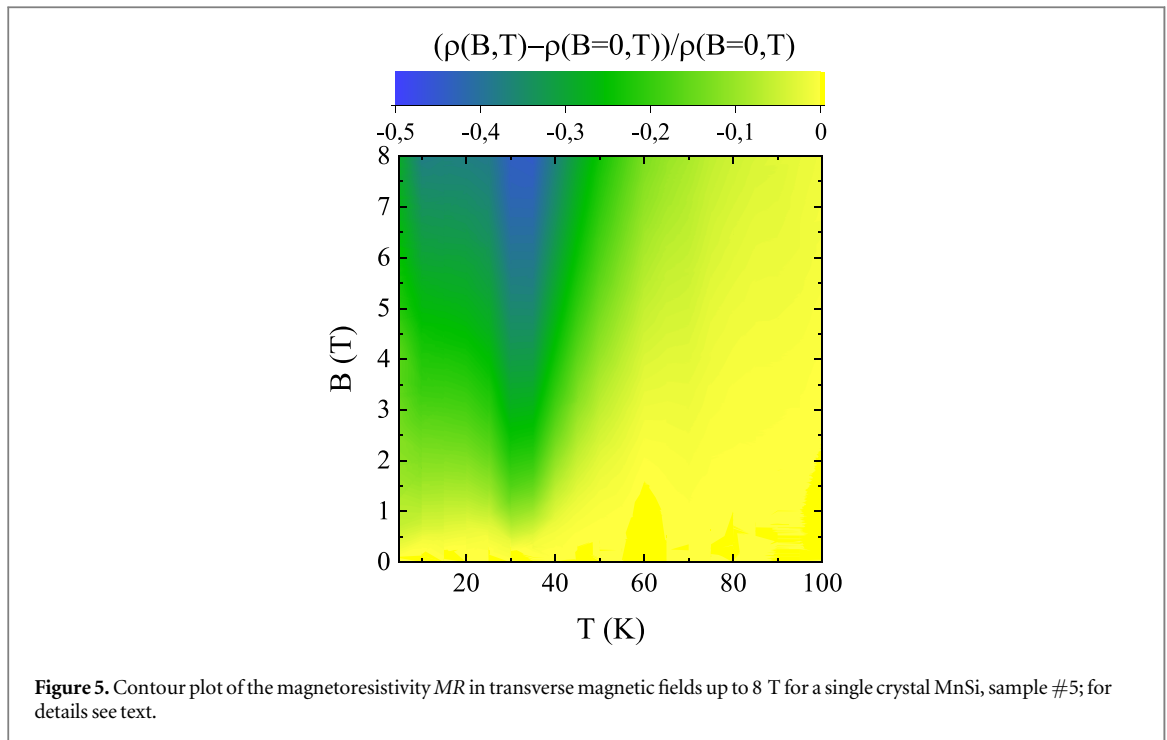


**Figure 4.** Contour plot of the magnetoresistivity  $MR$  in transverse and parallel magnetic fields up to 24 T for a 30 nm thin film MnSi; for details see text.

illustrate this effect is to present the data in form of contour plots, as we do in figure 4 for the data from figure 2, including here also the measurements for the parallel field alignment. In this representation, the color coding reflects the size of the magnetoresistivity, which nicely illustrates the most pronounced negative magnetoresistivity to occur close to  $T_N$ .

Interestingly, the contour plot demonstrates that there is some asymmetry in the magnetoresistivity. The  $MR$  is somewhat stronger at temperatures  $T < T_N$  than at  $T > T_N$ . If the  $MR$  would just reflect the suppression of spin fluctuations, one would naively argue that magnetic order already removes some of the spin fluctuations, as it is indicated by the downturn of the zero field resistivity at  $T_N$ . Then, for a normalized quantity as the  $MR$  this should show up as a comparatively smaller signal, if compared to a situation where no spin fluctuations have been removed in zero magnetic field. Therefore, the asymmetry would be expected to appear as a stronger  $MR$  above  $T_N$ , as it has been shown for instance for the itinerant weak ferromagnet  $NbFe_2$  [31].

In fact, corresponding magnetoresistivity measurements on single crystalline MnSi (now up to only 8 T) are more in line with the observations made for single crystalline  $NbFe_2$ . This is illustrated in figure 5, where we display a contour plot of the  $MR$  of sample #5 in the same fashion as the thin film data. Here, the asymmetry in



the magnetoresistivity is clearly tilted towards temperatures  $T > T_N$ , reflecting a stronger suppression of spin fluctuations in the paramagnetic phase. Altogether, while the overall magnetoresistive behavior of bulk and thin film material exhibits a strong resemblance, there seem to be residual subtle differences in some aspects. If these subtle differences are extrinsic or intrinsic is not entirely clear. It seems conceivable that a distribution of transition temperatures in the films causes a smearing of the magnetoresistive features towards lower temperatures, and thus would be the result of a somewhat larger structural inhomogeneity in films than in single crystals.

Finally, to illustrate the similar behavior seen for both our samples, in figure 6 we present the contour plots of the magnetoresistivity for the 10 nm film. Overall, there is a close similarity for all data sets, be it that the magnetoresistive effects are somewhat weaker for the 10 nm sample compared to the 30 nm film. This simply reflects the larger zero field resistivity of the 10 nm sample, which will reduce the overall signal size of the  $MR$  (see figure 1).

#### 4. Discussion

So far, experimentally we have demonstrated two points: (a.) There is basically no difference in the magnetoresistive response of films MnSi with different thickness and for different field directions. Thus, structurally the films are still in a 3D-limit, consistent with the argument that size effects induced by the film thickness only occur below  $\sim 10$  nm thickness [13]. As well, the negligible difference between longitudinal and transverse magnetoresistivity likely reflects the morphology of our films, i.e., epitaxial growth of MnSi islands with a typical diameter of  $\sim 50$  nm [29]. A significant scattering contribution will thus arise from the grain boundaries and surfaces, which are present for both experimental geometries. Conversely, effects such as the existence of skyrmions, domains, Fermi surface anisotropies etc. that might lead to a difference of longitudinal and transverse magnetoresistivity will only have a secondary relevance. (b.) On a qualitative and semi-quantitative level there is a close resemblance of the magnetoresistivity of thin film MnSi to that of single crystalline material. We thus can proceed and carry out a data analysis as has been put forth by Sakakibara *et al* [4].

We start by noting that for weakly and nearly ferromagnetic metals the in-field dependence of the low-temperature magnetoresistivity can be expressed as [32]  $R(T, B) = R_0 + R_2(B)T^2$ .  $R_0$  is the residual resistance at 0 K, while the second term reflects the spin fluctuation effect of an itinerant weakly or nearly ferromagnetic material. The factor  $R_2(B)$  of the spin fluctuation term can be determined from the  $MR$  data by plotting  $R(T, B) - R_0$  over  $T^2$ . In this representation, at low enough temperatures the quantity  $R(T, B) - R_0$  results in straight lines versus  $T^2$ , where the slope corresponds to  $R_2(B)$ . In figure 7 we plot the experimental data for the 10 nm film for selected magnetic fields in this representation, verifying that our approach to analyze the data

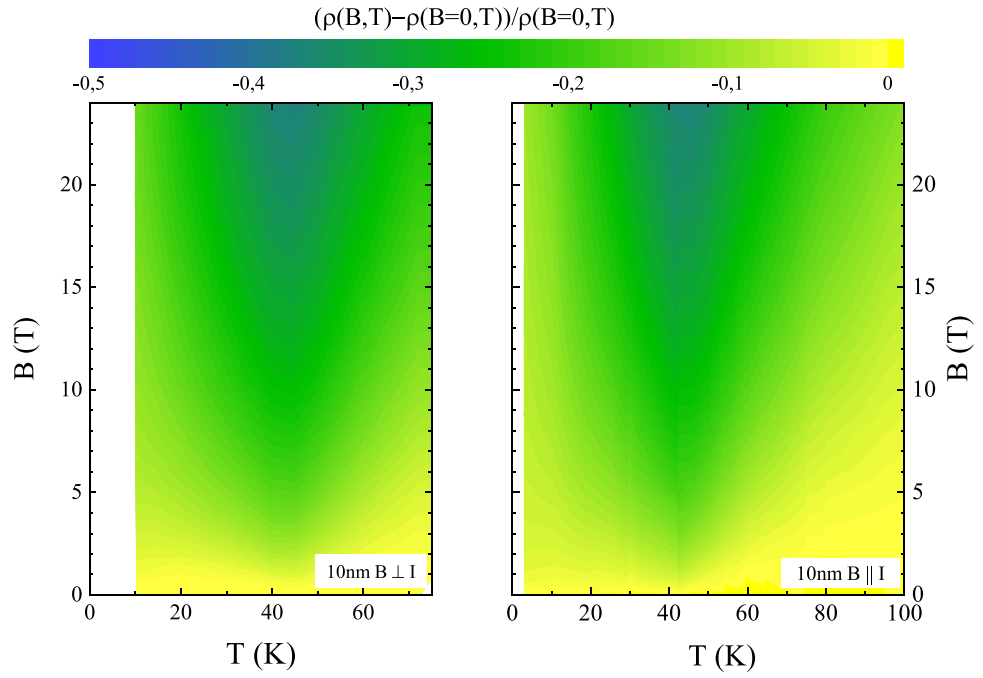


**Figure 6.** Contour plot of the magnetoresistivity  $MR$  in transverse and parallel magnetic fields up to 24 T for a 10 nm thin film MnSi; for details see text.

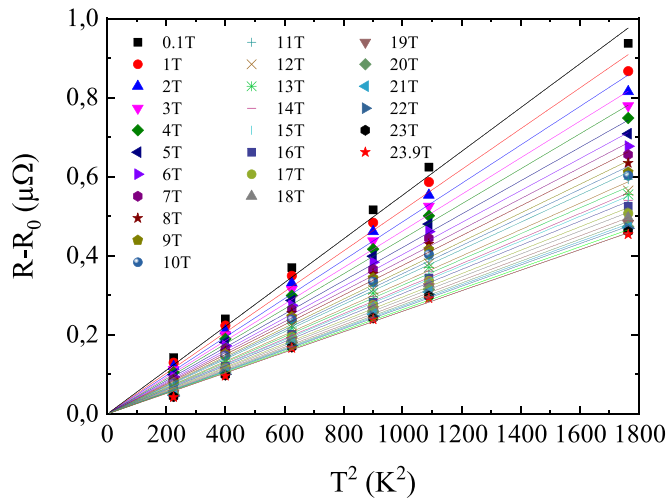


**Figure 7.** Plot for data analysis of the magnetoresistivity  $MR$  in parallel magnetic fields up to 24 T for a 10 nm thin film MnSi; for details see text.

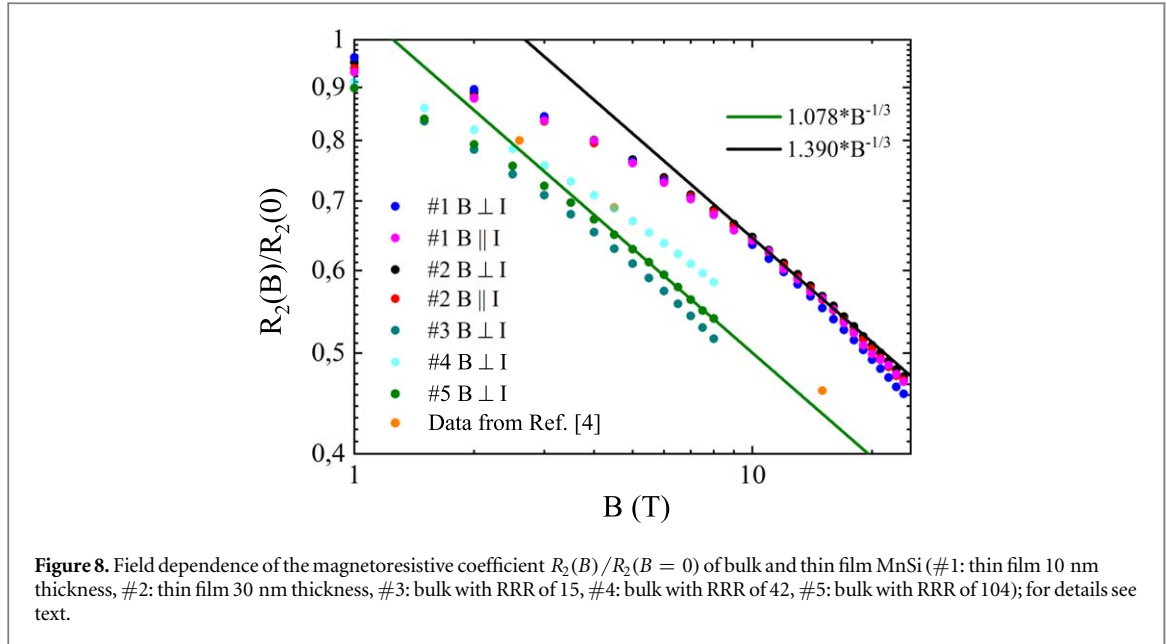
reproduces our experimental findings over a wide temperature range in a similar manner as presented in [4]. From linear fits of  $R(T, B) - R_0$  versus  $T^2$  in the temperature range below 30 K we thus obtain the quantity  $R_2(B)$ .

With respect to this type of analysis, since the residual resistivity  $R_{T,B=0}$  has a temperature dependence because of phonon scattering, strictly speaking we should plot  $R(T, B) - R(T, B = 0) \propto T^2$ . In fact, as a first approximation, allowing  $R_0$  as a free fitting parameter to vary by about 10 % slightly improves the fitting, but it does not affect the fundamental outcome of the data analysis, i.e., the field dependence  $R_2(B)$ .

Next, we follow the argumentation from [4] and plot the normalized field dependence of the resistive coefficient  $R_2(B)/R_2(B = 0)$  in figure 8. We include the data from our two thin film samples for both field geometries, from the single crystals measured as references, and the data from [4]. By plotting a normalized quantity, we circumvent the uncertainties in the determination of absolute resistivity values.

From the plot, it is immediately clear that overall thin film and single crystal samples exhibit a qualitatively similar behavior, while quantitatively there are clear differences. First, for single crystalline material, and even





under consideration of the limited field range for the crystals measured here, our data sets reproduce those from Sakakibara *et al* [4] on single crystalline samples. With the residual resistivity ratios for the crystals used for this plot varying by almost an order of magnitude, we conclude that disorder does not significantly affect the magnetoresistive behavior.

As was pointed out, in high fields the magnetoresistive behavior of a weakly or nearly ferromagnetic metal such as MnSi should have a field dependence evolving like  $R_2(B)/R_2(B = 0) \propto B^{-1/3}$  [4, 32]. The solid lines in figure 8 visualize such a field dependence, which to reasonable approximation is fulfilled both for single crystal and thin film MnSi in a similar high field range. Consequently, the magnetoresistive response of thin film MnSi can essentially be understood within what is nowadays labeled the self-consistent renormalization (SCR) theory of spin fluctuations [5]. Conversely, the quantitative difference between thin films and single crystals must reflect a difference of the microscopic parameters used within SCR theory to describe the spin fluctuations.

More specifically, by writing out the expressions for the high field magnetoresistivity given in [32], one finds that  $R_2(B)/R_2(B = 0)$  is a complex function of variables introduced in SCR theory to parametrize the spin fluctuations:  $R_2(B)/R_2(B = 0) \propto \sqrt{\frac{\chi_0}{\chi L^{1/3}}} B^{-1/3}$ , with  $\chi_0$  the susceptibility of the non-interacting system,  $\chi$  the susceptibility of the interacting system, and  $L$  an expansion coefficient of the magnetic free energy. Evidently, we cannot extract unique values for these parameters from our experiment, and thus cannot uniquely parametrize the quantitative difference between thin film and single crystal data within the language of SCR theory. However, we note that this difference cannot be attributed to the different magnetic transition temperatures, since SCR theory would predict that  $R_2(B)/R_2(B = 0) \propto \sqrt{T_N^{-1/3}} B^{-1/3}$ , i.e., a larger  $T_N$  should lead to a smaller prefactor, contrary to our observations.

At this point, we can only speculate about the microscopic origin of the different prefactors of the magnetoresistive coefficient  $R_2(B)/R_2(B = 0)$  in thin film and single crystalline MnSi. Possibly, it could be associated to the effective negative pressure in the thin films. Alternatively, the uni-axial anisotropy induced in the films, which was argued to substantially affect film properties [10, 19], might cause modifications of the spin fluctuation spectra. One way to test these notions would be—for instance—corresponding magnetoresistivity measurements under pressure on thin film MnSi. If the pressure scenario holds, we would expect a gradual transition of the magnetoresistive behavior of the films towards the bulk behavior with applied pressure [20].

Another line of arguments could be based on considering the assumptions of spin fluctuation theory. The theory starts out by describing the free energy of a material in terms of spin fluctuations. For a thin film sample, however, surface and interface contributions have to be included in the free energy. These might lead to quantitative changes to the behavior of a system, while there are no overall qualitative changes.

Altogether, we conclude that in terms of spin fluctuations thin film and bulk (single crystal) MnSi can be understood within the same SCR theoretical framework. Moreover, our findings imply that thin films are in a different spin fluctuation parameter range than bulk (single crystalline) material. The origin of this difference will need further exploration.



## Acknowledgments

We acknowledge fruitful discussions with U K Rössler. We acknowledge the support of the LNCMI-CNRS, member of the European Magnetic Field Laboratory (EMFL). We gratefully acknowledge support by the Braunschweig International Graduate School of Metrology B-IGSM and the DFG Research Training Group GrK1952/1 'Metrology for Complex Nanosystems'. We furthermore acknowledge support by the German Research Foundation and the Open Access Publication Funds of the Technische Universität Braunschweig.

## ORCID iDs

S Süllow  <https://orcid.org/0000-0001-8522-1360>

## References

- [1] Williams H J, Wernick J H, Sherwood R C and Wertheim G K 1966 *J. Appl. Phys.* **37** 1256
- [2] Shinoda D and Asanabe S 1966 *J. Phys. Soc. Jpn.* **21** 555
- [3] Pfeleiderer C, Adams T, Bauer A, Biberacher W, Binz B, Birkelbach F, Böni P, Franz C, Georgii R and Janoschek M 2010 *J. Phys.: Condens. Matter* **22** 164207
- [4] Sakakibara T, Morimoto H and Date M 1982 *J. Phys. Soc. Jpn.* **51** 2439
- [5] Moriya T 1985 *Spin Fluctuations in Itinerant Electron Magnetism (Solid-State Sciences)* (Berlin: Springer)
- [6] Thompson J D, Fisk Z and Lonzarich G G 1989 *Physica B* **161** 317
- [7] Mühlbauer S, Binz B, Jonietz F, Pfeleiderer C, Rosch A, Neubauer A, Georgii R and Böni P 2009 *Science* **323** 5916
- [8] Karhu E, Kahwaji S, Monchesky T L, Parsons C, Robertson M D and Maunders C 2010 *Phys. Rev. B* **82** 184417
- [9] Karhu E A, Kahwaji S, Robertson M D, Fritzsche H, Kirby B J, Majkrzak C F and Monchesky T L 2011 *Phys. Rev. B* **84** 060404(R)
- [10] Karhu E A, Rössler U K, Bogdanov A N, Kahwaji S, Kirby B J, Fritzsche H, Robertson M D, Majkrzak C F and Monchesky T L 2012 *Phys. Rev. B* **85** 094429
- [11] Geisler B, Kratzer P, Suzuki T, Lutz T, Costantini G and Kern K 2012 *Phys. Rev. B* **86** 115428
- [12] Wilson M N, Karhu E A, Quigley A S, Rössler U K, Butenko A B, Bogdanov A N, Robertson M D and Monchesky T L 2012 *Phys. Rev. B* **86** 144420
- [13] Engelke J, Reimann T, Hoffmann L, Gass S, Menzel D and Süllow S 2012 *J. Phys. Soc. Jpn.* **81** 124709
- [14] Li Y, Kanazawa N, Yu X Z, Tsukazaki A, Kawasaki M, Ichikawa M, Jin X F, Kagawa F and Tokura Y 2013 *Phys. Rev. Lett.* **110** 117202
- [15] Suzuki T, Lutz T, Geisler B, Kratzer P, Kern K and Costantini G 2013 *Surf. Sci.* **617** 106
- [16] Menzel D, Engelke J, Reimann T and Süllow S 2013 *J. Kor. Phys. Soc.* **62** 1580
- [17] Wilson M N, Karhu E A, Lake D P, Quigley A S, Meynell S, Bogdanov A N, Fritzsche H, Rössler U K and Monchesky T L 2013 *Phys. Rev. B* **88** 214420
- [18] Yokouchi T, Kanazawa N, Tsukazaki A, Kozuka Y, Kawasaki M, Ichikawa M, Kagawa F and Tokura Y 2014 *Phys. Rev. B* **89** 064416
- [19] Wilson M N, Butenko A B, Bogdanov A N and Monchesky T L 2014 *Phys. Rev. B* **89** 094411
- [20] Engelke J, Menzel D, Hidaka H, Seguchi T and Amitsuka H 2014 *Phys. Rev. B* **89** 144413
- [21] Meynell S A, Wilson M N, Fritzsche H, Bogdanov A N and Monchesky T L 2014 *Phys. Rev. B* **90** 014406
- [22] Meynell S A, Wilson M N, Loudon J C, Spitzig A, Rybakov F N, Johnson M B and Monchesky T L 2014 *Phys. Rev. B* **90** 224419
- [23] Yokouchi T, Kanazawa N, Tsukazaki A, Kozuka Y, Kikkawa A, Taguchi Y, Kawasaki M, Ichikawa M, Kagawa F and Tokura Y 2015 *J. Phys. Soc. Jpn.* **84** 104708
- [24] Lancaster T et al 2016 *Phys. Rev. B* **93** 140412(R)
- [25] Figueroa A I, Zhang S L, Baker A A, Chalasani R, Kohn A, Speller S C, Gianolio D, Pfeleiderer C, van der Laan G and Hesjedal T 2016 *Phys. Rev. B* **94** 174107
- [26] Meynell S A, Spitzig A, Edwards B, Robertson M D, Kalliecharan D, Kreplak L and Monchesky T L 2016 *Phys. Rev. B* **94** 184416
- [27] Meynell S A, Wilson M N, Krycka K L, Kirby B J, Fritzsche H and Monchesky T L 2017 *Phys. Rev. B* **96** 054402
- [28] Trabel M, Tarakina N V, Pohl C, Constantino J A, Gould C, Brunner K and Molenkamp L W 2017 *J. Appl. Phys.* **121** 245310
- [29] Schroeter D, Steinki N, Schilling M, Fernández Scarioni A, Krzysteczko P, Dziomba T, Schumacher H W, Menzel D and Süllow S 2018 *J. Phys.: Condens. Matter* **30** 235805
- [30] Adams T et al 2011 *Phys. Rev. Lett.* **107** 217206
- [31] Rauch D, Steinki N, Knafo W, Pfeleiderer C, Duncan W J, Grosche F M and Süllow S 2018 *Physica B* **536** 510
- [32] Ueda K 1976 *Solid State Commun.* **19** 965